



CHORUS

This is the accepted manuscript made available via CHORUS. The article has been published as:

# Hierarchy of anomalies in the two-dimensional Mercedes-Benz model of water

Tomaz Urbic and Ken A. Dill

Phys. Rev. E **98**, 032116 — Published 11 September 2018

DOI: [10.1103/PhysRevE.98.032116](https://doi.org/10.1103/PhysRevE.98.032116)

# Hierarchy of anomalies in the two-dimensional Mercedes–Benz model of water

Tomaz Urbic\*

*University of Ljubljana, Faculty of Chemistry and Chemical Technology,  
Večna pot 113, SI-1000 Ljubljana, Slovenia*

Ken A. Dill

*Laufer Center for Physical and Quantitative Biology,  
Stony Brook University, Stony Brook, NY 11794-5252*

## Abstract

We investigate by Monte Carlo simulations density, diffusion and structural anomalies of the simple two dimensional Mercedes–Benz (MB) model of water, which is a very simple toy model for explaining the origin of water properties. MB water molecules are modeled as two-dimensional Lennard-Jones disks, with three orientation-dependent hydrogen-bonding arms, arranged as in the MB logo. The model is in a way also variance of silica-like models. Beside the know thermodynamic anomaly for the model we also found diffusion and structural anomalies and map out the cascade of density, structural, pair entropy and diffusivity anomalies for MB model. The orientational order parameters with three and six fold symmetry were determined and maximum for each observed. The anomalies occur in hierarchy order which is slight variation of hierarchy order in real water. The diffusion anomaly region is the innermost in the hierarchy while for water is density anomaly region.

---

\*Electronic address: [tomaz.urbic@fkkt.uni-lj.si](mailto:tomaz.urbic@fkkt.uni-lj.si)

## I. INTRODUCTION

Anomalous liquids are liquids that exhibit unexpected behavior upon variations of the thermodynamic conditions in comparison to normal (argon-like) liquids. Water is the classic example of those anomalous liquids. There are two very distinct mechanisms that give rise to the anomalous properties. Angular-dependent interactions, such as oriented hydrogen bonding in water, tetrahedral bonding in silica, [1–3] and oriented bonds in  $\text{BeF}_2$ , can result in density maximum because of the competition between tetrahedral order (low density) and translational order (high density). On the other hand, density anomaly was also observed for Ga[4], Bi[5], Te [6], S [7], Be, Mg, Ca, Sr, Ba, P, Se, Ce, Cs, Rb, Co, Ge where system lacks oriented bonding. Speaking of water, it expands upon cooling at fixed pressure, diffuses faster upon compression at fixed temperature[8, 9], and becomes less ordered upon increasing density at constant temperature[10]. These are the density, diffusion, and structural anomalies. Regions, in which these anomalies occur, form nested domes in the density-temperature diagram[10] or pressure-temperature diagram[11]. The structural anomaly domain occupies the outer region of the pressure temperature phase diagram and the density anomaly region is the innermost region for water like fluids. The diffusion anomaly region lies between these two domains [10, 11]. This is called the hierarchy of water anomalies. It must be noted, however, that for different compounds not all anomalies always appear and that detailed understanding of their origin and their hierarchy remain elusive[12, 13].

A large number of models of varying complexity have been developed and analyzed to model waters extraordinary properties, for reviews, see, e.g. [14–17]. Many properties of water and aqueous solutions can be captured by simpler models[18, 19]. One class of such simpler models has been developed by Nezbeda and coworkers[15, 20, 21], There are also many other simple models[22–26]. One the simplest model for water is the so-called Mercedes-Benz (MB) model[27–31] which was originally proposed by Ben-Naim in 1971 [32, 33]. This is a 2-dimensional toy model where each water molecule is modeled as a disk that interacts with other such waters through: (1) a Lennard-Jones (LJ) interaction and (2) an orientation-dependent hydrogen bonding interaction through three radial arms arranged as in the Mercedes-Benz (MB) logo. Interest in simplified models is due to insights that are not obtainable from all-atom computer simulations. Simpler models are more flexible in providing insights and illuminating concepts, and they do not require big computer re-

sources. Second, the simple models can explore a much broader range of conditions and external variables. Whereas simulating a detailed model may predict the behavior at one temperature and pressure, a simpler model can be used to study a whole phase diagram of temperatures and pressures. Third, the analytical models can provide functional relationships for engineering applications and lead to improved models of greater computational efficiency. Fourth, simple models can be used as a polygon to develop and study theoretical methods. Our interest in using the MB is that it serves as one of the simplest models of an orientationally dependent liquid, so it can serve as a testbed for developing analytical theories that might ultimately be useful for more realistic models. Another advantage of the MB model, compared to the more realistic water models, is that the underlying physical principles can be more readily explored and visualized in two dimensions. For MB model, the NPT Monte Carlo simulations have shown that the MB model predicts qualitatively the density anomaly, the minimum in the isothermal compressibility as a function of temperature, the large heat capacity, as well as the experimental trends for the thermodynamic properties of solvation of nonpolar solutes[28, 30, 31, 34] and cold denaturation of proteins[35]. The 2D MB model was also extended to 3D by Bizjak et al.[36, 37] and Dias et al.[34, 38] and studied using computer simulations [34, 36–38]. The 2D model was also extensively studied with analytical methods like integral equation and thermodynamic perturbation theory[39–45].

In this paper, we investigate the presence of the anomalies in a simple 2D MB model of water in Fig. 1. We determined the density, diffusion, and structural anomalies and we observe that they occur with hierarchy slightly different as in water. The outline of the paper is as follows. We present the MB model in Sec. II, and the details of the Monte Carlo simulations in Sec. III. In Sec. IV we show and discuss the results and summarize everything in Sec. V.

## II. THE MODEL

In the framework of the MB model of water the water molecules are modelled as a two-dimensional disk with three bonding arms separated by an angle of  $120^\circ$ [28, 32] which is fixed. These arms mimic formation of hydrogen bonds. The interaction potential between water particles  $i$  and  $j$  is a sum of a Lennard–Jones (LJ) and a hydrogen–bonding (HB)

term

$$U(\vec{X}_i, \vec{X}_j) = U_{LJ}(r_{ij}) + U_{HB}(\vec{X}_i, \vec{X}_j) \quad (1)$$

$r_{ij}$  is distance between centers of particles  $i$  and  $j$ .  $\vec{X}_i$  and  $\vec{X}_j$  are the vectors representing the coordinates and the orientation of the  $i^{th}$  and  $j^{th}$  molecule. The Lennard–Jones part of the potential has a standard form

$$U_{LJ}(r_{ij}) = 4\varepsilon_{LJ} \left( \left( \frac{\sigma_{LJ}}{r_{ij}} \right)^{12} - \left( \frac{\sigma_{LJ}}{r_{ij}} \right)^6 \right), \quad (2)$$

$\varepsilon_{LJ}$  is the depth and  $\sigma_{LJ}$  the contact value. The hydrogen bonding part of the potential is sum of interactions  $U_{HB}^{kl}$  between all arms of different molecules

$$U_{HB}(\vec{X}_i, \vec{X}_j) = \sum_{k,l=1}^3 U_{HB}^{kl}(r_{ij}, \theta_1, \theta_2). \quad (3)$$

This interaction is described by Gaussian function in distance and both angles

$$U_{HB}^{kl}(r_{ij}, \theta_1, \theta_2) = \varepsilon_{HB} G(r_{ij} - r_{HB}) G(\vec{i}_k \vec{u}_{ij} - 1) G(\vec{j}_l \vec{u}_{ij} + 1) \quad (4)$$

$$= \varepsilon_{HB} G(r_{ij} - r_{HB}) G(\cos(\theta_i + \frac{2\pi}{3}(k-1)) - 1) G(\cos(\theta_j + \frac{2\pi}{3}(l-1)) + 1) \quad (5)$$

$\varepsilon_{HB} = -1$  is a HB energy parameter and  $r_{HB} = 1$  is a characteristic length of hydrogen bond.  $\vec{u}_{ij}$  is the unit vector along  $\vec{r}_{ij}$  and  $\vec{i}_k$  is the unit vector representing the  $k^{th}$  arm of the  $i^{th}$  particle.  $\theta_i$  is the orientation of  $i^{th}$  particle with respect to  $x$  axes.  $G(x)$  is an unnormalized Gaussian function

$$G(x) = \exp\left(-\frac{x^2}{2\sigma^2}\right). \quad (6)$$

The strongest hydrogen bond occurs when an arm of one particle is co-linear with the arm of another particle and the two arms point in opposing directions. The LJ well-depth  $\varepsilon_{LJ}$  is 0.1 times the HB interaction energy  $\varepsilon_{HB}$  and the Lennard–Jones contact parameter  $\sigma_{LJ}$  is  $0.7r_{HB}$ . The width of Gaussian for distances and angles ( $\sigma = 0.085r_{HB}$ ) is small enough that a direct hydrogen bond is more favorable than a bifurcated one.

### III. MONTE CARLO COMPUTER SIMULATION

In order to determine anomalies and their hierarchy in the 2D MB model of water we performed Monte Carlo computer simulations in canonical ensemble (constant  $N$ ,  $V$ , and

T)[46, 47]. In order to mimic an infinite size of system of particles we used the periodic boundary conditions and the minimum image convention. All starting configurations were selected at random. Each move consisted of translation of random particle and rotation of different random particle. Probabilities for translation and rotation were the same. In one cycle (also one time step) we tried to translate and rotate each particle once on average. The simulations were equilibrated for 5000000 cycles and averages were taken for 20 series each consisted for another 5000000 cycles to obtain well converged results. In the system we had from 100 to 500 particles depending on density of the system. We used such number of particles that increase of this number had no significant effect on the calculated quantities. The system of 100 molecules in 2D is equivalent to 1000 particles in 3D although 2D systems are more complicated in comparison to 3D. It is well-known that when confined to 2D space, condensed matter behaves differently than in 3D. An example is provided by 2D crystals, where thermal fluctuations are so strong as to rule out long-range translational order for non-zero temperatures, leaving it open for the possibility of unconventional melting scenarios[48]. Thermodynamic quantities such as energy were calculated as statistical averages over the course of the simulations [47]. Cut off of the potential was half-length of the simulation box. The pressure was calculated by means of virial equation [47].

The diffusion coefficient is determined using the mean square displacement averaged over different series. In these MC simulation runs, dynamic adjustment of maximum displacement was turned off and was kept fixed for all instances. The mean square displacement was calculated as average of displacements over all particles

$$\langle \Delta r(n)^2 \rangle = \langle (\vec{r}(n) - \vec{r}_0)^2 \rangle \quad (7)$$

where  $\vec{r}_0$  is initial coordinate of the particle and  $n$  is number of cycle. The pseudo diffusion coefficient which is proportional to real diffusion coefficient was obtained as

$$D^* = \lim_{n \rightarrow \infty} \frac{\langle \Delta r(n)^2 \rangle}{n} \quad (8)$$

It is well known this latter quantity may be ill defined in a 2D system because of the possible existence of a long-time (1/t) tail in the velocity auto-correlation function [49]. The quantity might be strongly sensitive to the size dependence. In our case we tested results by increasing number of particles times two and times three and in each cases results were in agreement. For normal pseudo-diffusion coefficient decreases monotonically with

increasing density at constant temperature. For MB model of water there is a region where the coefficient increases.

Structural anomaly was assessed by determining translational order parameter  $t$  and two orientational order parameters (with three fold symmetry,  $q_3$  and with six-fold symmetry,  $q_6$ ). The translational order parameter measures the degree of pair correlation in the system and is defined as

$$t = \int_0^{x_c} |g(x) - 1| dx \quad (9)$$

where  $x = \rho^{\frac{1}{2}}r$  is the distance  $r$  in the units of mean inter-particle separation and  $g(x)$  the pair distribution function.  $x_c$  is the cut off distance and is set to half of the simulation box in the present paper. For normal fluids translational order parameter monotonically increases with density. If a different behavior is observed in a certain density range, the fluid is said to exhibit a structural anomaly. Orientational order parameters,  $q_l$  we calculated following this procedure. For each particle  $j$  we calculate

$$q_l^j = \frac{1}{n_j} \sum_k \exp(il\theta_{jk}) \quad (10)$$

where  $n_j$  is the number of neighbors within the first atom shell of particle  $j$  and  $\theta_{jk}$  is the angle between the vector connecting particles  $j$  and  $k$  and the horizontal axis. Parameter  $l$  specifies the type of symmetry (3 or 6). The local orientational parameter of the whole system is calculated as average of absolute value over all the particles in the system

$$q_l = \frac{1}{N} \sum_{i=1}^N |q_l^i|. \quad (11)$$

The excess entropy is a convenient quantity for understanding the links between structure and thermodynamics, as well as dynamics. To calculate the excess entropy we should count all the accessible configurations for a fluid and compare it with the ideal gas entropy. The excess entropy can also be calculated by the multiparticle correlation expansion

$$s_e = s_2 + s_3 + \dots + s_n + \dots \quad (12)$$

where  $s_n$  denotes the entropy contribution due to  $n$ -particle correlations. The effect of triplet and higher-order correlations on the entropy has not been extensively studied, the pair entropy itself proves to be a very convenient structural estimator for the entropy. The pair entropy can be approximated by

$$s_2 = -\pi\rho \int (g(r) \ln g(r) - g(r) + 1) r dr \quad (13)$$

and is dominant contribution to excess entropy[50–60]. Integration was up to half length of simulation box. The pair entropy is proved to be between 85% and 95% of the total excess entropy in Lennard-Jones systems[51]. At higher temperatures we determine excess entropy by Widom method and we observed similar agreement for MB model as reported for LJ systems. The pair entropy only depends on the pair correlation function  $g(r)$  and the density and it is related to the translational order parameter because both are related to deviation of radial distribution function from unity.

#### IV. RESULTS AND DISCUSSION

All our results were calculated and are reported in reduced units; the excess internal energy and temperature are normalized to the HB energy parameter  $\varepsilon_{HB}$  ( $A^* = \frac{A}{|\varepsilon_{HB}|}$ ,  $T^* = \frac{k_B T}{|\varepsilon_{HB}|}$ ) and the distances are scaled to the hydrogen bond characteristic length  $r_{HB}$  ( $r^* = \frac{r}{r_{HB}}$ ). Errors in the MC simulations depend on temperature, for most of the temperatures are of size of the symbols used to present data points.

2D MB model of water has water-like behavior as reported before [28]. Density of low density ice (see Figure 2) is lower than density of liquid phase. Two most important crystal phases of 2D MB water are low density crystal with reduced density 0.7698 where water molecules occupy positions in hexagonal lattice. There is only one possible crystalline arrangement that permits the maximum number of perfect hydrogen bonds per molecule. This low-density crystal structure is analogous to hexagonal ice Ih, and it is also the crystalline phase that has been observed in low temperature Monte Carlo simulations of the MB model[28]. The 2D MB water also has denser forms of ice at high pressures. One possible candidate for high density crystal phase is where another water molecule occupy empty spaces in hexagons (see Figure 2). This phase conforms to triangular packing arrangement. Reduced density of high density crystal phase is 1.1547. We should take into account that the two ices described above do not exhaust the possible crystalline structures for this model. When the MB water melts, the structure of low density ice is present a lot also in liquid water. Figure 3 shows phase diagram of MB model since the freezing (melting) coexistence lines are relevant to locate if some thermodynamic points fall in the metastable regions of the model. As we can see from the phase diagram the anomalous regions are present in fluid part of phase diagram and extend also in supercooled region.

First we determine density anomaly. We can this by calculating the density as function of temperature at constant pressure and observe density maximum at certain pressures. This was done for selected pressures before [28]. There is an alternative way to determine temperature of maximum density. This is by calculating pressure as function of density at constant temperature. Where density maximum is present we observe minimum in pressure as a function of density. Several isochores are presented in Figure 4. as well as a line showing temperatures of maximum density. For the model we observe density anomaly for the temperatures lower than 0.18 and for the densities between 0.8 and 1.1 and for the pressures between 0.05 and 0.3. This is in a small region between density of low and high crystal phases. The origin of density anomaly is that at lower temperatures water still has a lot of low density ice structure present in the liquid phase. These structures are melting. Water molecules which are released from crystal structures occupy empty spaces between hexagons and the density of liquid increases. Upon further increase of temperature hydrogen bonds continue to melt and more opened structures are formed which has lower density. At higher temperature such crystal water structures are no present and there is no density anomaly. Water behaves as a normal liquid where density decrease with increase of temperature at constant pressure.

We continue our calculation by determining the density anomaly. We calculated the pseudo diffusion coefficient by the displacement of water molecules in the MC steps at fixed maximum step. This pseudo diffusion coefficient is proportional to real diffusion coefficient of the 2D MB model. For normal fluids diffusivity decreases monotonically with increasing density at constant temperature because with increase of density there is more crowding and molecules move with higher difficulty. For 2D MB model this is observed only for temperatures higher than 0.175. For temperatures lower than 0.175 diffusion has anomalous behavior. At first the diffusion decreases, reaches minimum, increases up to maximum and decreases toward zero for high densities. The region between the minimum and the maximum is so-called anomalous diffusion region and is presented in Figure 5. This anomaly region is also present in the density range between the high and low density ices. As the density increases at constant temperature the water form more correct hexagonal network and a little after density of low density crystal phase diffusion has minimum. Upon further increase of the density water molecules occupy empty space within the hexagons and diffusion start to increase since these molecules are less bonded than molecules forming HB networks and

can move easier. Upon further increase of the density the system reaches such density that mobility of molecules reach maximum and upon further increase less and less space is available and molecules move with bigger difficulty and diffusion starts to decrease. What is unexpected is that this diffusion anomalous region lies within the density anomalous region. In water like models and in silica like models density anomalous region is most inner region. The reason for this is no completely clear, one reason might be the dimensionality of the system. Here we have the 2D model with water-like properties or we can have model that is not completely water or silica like but has its unique properties. Since the diffusion is related with ability of water molecules to move we plotted in Figure 6 ratio of differently bonded water molecules. We would expect that when diffusion of water is smaller that water molecules would be strongly bonded or on the other hand would not have available space where to move. We would expect some unusual behavior, but contrary these properties does not have anything unusual. All functions are monotonic function with respect to temperature so they do not give us any new insight in reason for diffusion anomaly with respect to strong bonding.

As third we studied the structural behavior by calculating three different quantities, the translational order parameter  $t$  and two orientational order parameters,  $q_3$  orientational order with three fold axis and  $q_6$  orientational order with six fold axis. For the normal fluids,  $t$  increases with increasing density. For the 2D MB model we found this monotonic behavior only for the temperatures higher that 0.19 (see Figure 7). For lower temperatures we observe that the  $t$  has a maximum, decreases up to a minimum and recovers the normal increasing behavior after the minimum. The region between the minimum and maximum is called the anomalous structure region. Figure 8 shows distribution of both orientational order parameters for low and high temperatures for different densities. We can see that at the densities close to the density of the low density ice we can see huge peak for three fold symmetry. Upon the increase of density we can see that other structures start to appear. We can observe additional peaks in distribution. Our study reveals the anomalous behavior also for both orientational order parameters. For the temperatures higher that 0.16 both parameters decrease with increase of density. For temperatures lower that 0.16 we can observe maximum close to density of low density ice phase. This is presented in Figure 9.

The order map in the  $t-q_3$  and  $t-q_6$  plane plotted in Figure 10 resembles the one observed for water and other two-scale potentials reported before [10–13]. There are two different

regimes present for both plots. For the temperatures belonging to the structural anomalous region we can observe curves to form closed loops while for higher temperatures curves turn in opposite direction without forming closed loops for both orientational parameters.

The region of entropy anomaly is given by the condition that the entropy of the liquid increases on compression. Maxwells relation relates the condition for entropy anomaly to the isothermal compressibility and the sign of the thermal expansion coefficient

$$\left(\frac{\partial s}{\partial \rho}\right)_T = -V^2 \frac{\alpha}{\kappa_T}. \quad (14)$$

The relation shows that the entropy displays anomalous behavior in the region where the thermal expansion coefficient is negative. Since for a classical fluid  $s = s_{id} + s_e$ , where  $s_{id}$  is the ideal gas entropy that has a monotonic dependence on the density, the condition for excess entropy anomaly corresponds to  $(\partial s_e / \partial \rho)_T > 0$ . The multiparticle correlation approximation expands the excess entropy as  $s_e = s_2 + s_3 + \dots + s_n$ , so it may be expected that if the pair correlations dominate the entropy of the liquid, the pair entropy would provide an equivalent condition for finding the region of entropy anomaly and this is what we did. In Figure 11 we plotted pair entropy as function of density and temperature and we observed anomalous region. In Figure 12 we plotted pair correlation functions for two different temperatures for several densities to try and see what might be the reason for anomalies. We can see that at low temperature there is long range structure change and we believe this is the reason for anomalies, but it does not give us insight on the hierarchy of them.

In Figure 13 we plotted the relation between the several anomalies presented for the 2D MB model of water. The errors of the quantities are of size of the symbols. The temperature of maximum density line lies between diffusion and entropy anomaly. There is difference between position of structure and entropy anomaly. Hierarchy of anomalies found here is different that reported for the SPC/E water, other two-scale potentials[10–13, 61] and a double-Gaussian fluid[62]. Prestipino et al.[63] have shown that the anomalous thermodynamic behavior may occur also for weakly softened potentials, i.e., simple fluids characterized by a repulsion that is only marginally softened and yields a single structure at a local level. The most inner is diffusion anomaly, then density and then structural. In water like hierarchy we have density,diffusion and structural while in silica like hierarchy we have density, structural and diffusion. Why 2D MB model has different hierarchy might be

related to dimensionality or combination of different effects. For the a coarse-grained model of a water monolayer between hydrophobic walls at partial hydration, the density anomaly is included in the diffusion anomaly region, as in water[64]. For an associating lattice gas (ALG) model which combines a two-dimensional lattice gas with particles interacting through a soft core potential and orientational degrees of freedom[65], the diffusion anomaly is included in the density anomaly region, as in the present model. A similar hierarchy has been found also for models in 3D[66] although never observing also the structural anomaly.

## V. CONCLUSIONS

The Monte Carlo simulations were used to predict the hierarchy of anomalies in the 2D MB model of water. The MB model balances the Lennard-Jones interactions with an orientation-dependence that is intended to mimic hydrogen-bonding. The MB model has previously been shown to have the volume anomalies of pure water and the thermal anomalies of nonpolar solvation. Beside the known density anomaly it was discovered that the MB model also has the structure and diffusion anomalies. The diffusion anomaly has the smaller region and is encompassed by the density anomalous region and this one by the structure anomalous region. This is slightly different as in the real water where the anomalies are in order of density, diffusion and structure or in the silica-like models where the anomalies are in order of density, structure and diffusion.

### Acknowledgments

This work was supported by the NIH (GM063592) and Slovenian Research Agency (P1 0103-0201, N1-0042) and the National Research, Development and Innovation Office of Hungary (SNN 116198).

- 
- [1] R. Sharma, S. N. Chakraborty, C. Chakravarty, *J. Chem. Phys.* **125**, 204501 (2006).
  - [2] M. S. Shell, P. G. Debenedetti, A. Z. Panagiotopoulos, *Phys. Rev. E* **66**, 056703 (2002).
  - [3] P. H. Poole, M. Hemmati, C. A. Angell, *Phys. Rev. Lett.* **79**, 2281 (1997).
  - [4] J.M. Kincaid, G. Stell, *Phys. Lett. A* **65**, 131 (1978).

- [5] P. Lamparter, S. Stieb, W. Knoll, Z. Naturforsch. A **31**, 90 (1976).
- [6] H. Thurn, J. Ruska, J. Non-Cryst. Solids **22**, 331 (1976).
- [7] G.E. Sauer, L.B. Borst, Science **158**, 1567 (1967).
- [8] C. A. Angell, E. D. Finch, P. Bach, J. Chem. Phys. **65**, 3063 (1976).
- [9] F.X. Prielmeier, E.W. Lang, R.J. Speedy, H.-D. Ludemann, Phys. Rev. Lett. **59**, 1128 (1987).
- [10] J. R. Errington, P.G. Debenedetti, Nature (London) **409**, 318 (2001).
- [11] P.A. Netz, F.W. Starr, H.E. Stanley, M.C. Barbosa, J. Chem. Phys. **115**, 344 (2001).
- [12] A. B. de Oliveira, G. Franzese, P. A. Netz, M. C. Barbosa, J. Chem. Phys. **128**, 064901 (2008).
- [13] G. Franzese, G. Malescio, A. Skibinsky, S. V. Buldyrev, H. E. Stanley, Nature (London) **409**, 692 (2001).
- [14] W. L. Jorgensen, J. Chandrasekhar, J. D. Madura, R. W. Impey, and M. L. Klein, J. Chem. Phys. **79**, 926 (1983).
- [15] I. Nezbeda, J. Mol. Liq. **73/74**, 317 (1997).
- [16] B. Guillot, J. Mol. Liq. **101**, 219 (2002).
- [17] C. Vega, J. L. F. Abascal, M. M. Conde, and J. L. Aragones, Faraday Discuss. **141**, 251 (2009).
- [18] T.M. Truskett, P.G. Debenedetti, S. Sastry, and S. Torquato, J. Chem. Phys. **111**, 2647 (1999).
- [19] K.A. Dill, T.M. Truskett, V. Vlachy, and B. Hribar-Lee, Ann. Rev. Biophys. Biomolec. Struc. **34**, 173 (2005).
- [20] I. Nezbeda, J. Kolafa and Yu. V. Kalyuzhnyi, Mol. Phys. **68**, 143 (1989).
- [21] I. Nezbeda and G. A. Iglesias-Silva, Mol. Phys. **69**, 767 (1990).
- [22] A. L. Balladares, V. B. Henriques and M. C. Barbosa, J. Phys.: Condens. Matter **19**, 116105 (2007).
- [23] M. Girardi, M. Szortyka and M. C. Barbosa, Physica A **386**, 692 (2007).
- [24] M. M. Szortyka, C. E. Fiore, V. B. Henriques, and M. C. Barbosa, J. Chem. Phys. **133**, 104904 (2010).
- [25] G. Franzese and H. E. Stanley, J. Phys.: Condens. Matter **14**, 2201 (2002).
- [26] V. Bianco and G. Franzese G. Sci. Rep. **4**, 4440 (2014).
- [27] G. Andoloro and R. M. Sperandeo-Mineo, Eur. J. Phys. **11**, 275 (1990).
- [28] K. A. T. Silverstein, A. D. J. Haymet and K. A. Dill, J. Am. Chem. Soc. **120**, 3166 (1998).

- [29] K. A. T. Silverstein, K. A. Dill, and A. D. J. Haymet, *Fluid Phase Equilibria* **120**, 3166 (1998).
- [30] N. T. Southall and K. A. Dill, *J. Phys. Chem. B* **104**, 1326 (2000).
- [31] K. A. T. Silverstein, A. D. J. Haymet and K. A. Dill, *J. Chem. Phys.* **114**, 6303 (2001).
- [32] A. Ben-Naim, *J. Chem. Phys.* **54**, 3682 (1971).
- [33] A. Ben-Naim, *Mol. Phys.* **24**, 705 (1972).
- [34] C. L. Dias, T. Hynninen, T. Ala-Nissila, A. S. Foster and M. Karttunen, *J. Chem. Phys.* **134**, 065106 (2011).
- [35] C. L. Dias, *Phys. Rev. Lett.* **109**, 048104 (2012).
- [36] A. Bizjak, T. Urbic, V. Vlachy, and K. A. Dill, *Acta Chim. Slov.* **54**, 532 (2007).
- [37] A. Bizjak, T. Urbic, V. Vlachy and K. A. Dill, *J. Chem. Phys.* **131**, 194504 (2009).
- [38] C. L. Dias, T. Ala-Nissila, M. Grant and M. Karttunen, *J. Chem. Phys.* **131**, 054505 (2009).
- [39] T. Urbic, V. Vlachy, Yu. V. Kalyuzhnyi, N. T. Southall and K. A. Dill, *J. Chem. Phys.* **112**, 2843 (2000).
- [40] T. Urbic, V. Vlachy, Yu. V. Kalyuzhnyi, N. T. Southall and K. A. Dill, *J. Chem. Phys.* **116**, 723 (2002).
- [41] T. Urbic, V. Vlachy, Yu. V. Kalyuzhnyi and K. A. Dill, *J. Chem. Phys.* **118**, 5516 (2003).
- [42] T. Urbic, V. Vlachy, O. Pizio, K. A. Dill, *J. Mol. Liq.* **112**, 71 (2004).
- [43] T. Urbic, V. Vlachy, Yu. V. Kalyuzhnyi and K. A. Dill, *J. Chem. Phys.* **127**, 174511 (2007).
- [44] T. Urbic and M. F. Holovko, *J. Chem. Phys.* **135**, 134706 (2011).
- [45] T. Urbic, *Phys. Rev. E* **96**, 032122 (2017).
- [46] J. P. Hansen and I. R. McDonald, *Theory of Simple Liquids* (Academic, London, 1986).
- [47] D. Frenkel and B. Smit, *Molecular simulation: From Algorithms to Applications*, (Academic Press, New York, 2000).
- [48] S. Prestipino, F. Saija and P. V. Giaquinta, *J. Chem. Phys.* **137**, 104503 (2012).
- [49] P. J. Camp, *Phys. Rev. E*, **71**, 031507 (2005).
- [50] H. J. Raveche, *J. Chem. Phys.* **55**, 2242 (1971).
- [51] A. Baranyai and D. J. Evans, *Phys. Rev. A* **40**, 3817 (1989).
- [52] H. S. Green, *The Molecular Theory of Fluids*, (North-Holland, Amsterdam, 1952).
- [53] Y. Rosenfeld, *J. Phys.: Condens. Matter* **11**, 5415 (1999).
- [54] J. Mittal, *J. Chem. Phys.* **125**, 076102, (2006).
- [55] J. Mittal, J. R. Errington, and T. M. Truskett, *J. Phys. Chem. B* **110**, 18147 (2006).

- [56] S. N. Chakraborty and C. Chakravarty, Phys. Rev. E **76**, 011201 (2007).
- [57] A. Scala, F. W. Starr, E. La Nave, F. Sciortino and H. E. Stanley, Nature **406**, 166 (2000).
- [58] M. Agarwal, R. Sharma, and C. Chakravarty, J. Chem. Phys. **127**, 164502 (2007).
- [59] M. Agarwal, and C. Chakravarty, J. Phys. Chem. B **111**, 13294 (2007).
- [60] P. Vilaseca and G. Franzese, J. Chem. Phys. **133**, 084507 (2010).
- [61] P. Vilaseca and G. Franzese, Journal of Non-Crystalline Solids **357**, 419 (2011).
- [62] S. Prestipino, C. Speranza, G. Malescio and P. V. Giaquinta, J. Chem. Phys. **140**, 084906 (2014)
- [63] S. Prestipino, F. Saija, and G. Malescio, J. Chem. Phys. **133**, 144504 (2010).
- [64] F. de los Santos and G. Franzese, J. Phys. Chem. B **115** 14311 (2011).
- [65] M. M.Szortyka and M. C. Barbosa, Physica A **380**, 27 (2007).
- [66] P. A. Netz, S. V. Buldyrev, M. C. Barbosa and H. E. Stanley, Phys. Rev. E **73**, 061504 (2006).

## CAPTIONS TO THE FIGURES.

**Figure 1.** The MB molecules. Particles form the strongest hydrogen bond when the arms are co-linear and the distance between the two particles is equal to  $r_{HB}$ .

**Figure 2.** (a) The unit cell of the low density ice. (b) The unit cell of the high density ice.

**Figure 3.**  $T^* - p^*$  phase diagram from MC simulations. Red curve are results for gas-liquid coexistence by Urbic [45] in comparison with prediction of phase diagram by Silverstain et al.[29] which is plotted by black line.

**Figure 4.** (a) The pressure as a function of temperature for different densities. Red lines correspond to isochores from bottom up for densities 0.8, 0.825, 0.85, 0.875, 0.9, 0.925, 0.95, 0.975, 1.0, 1.025, 1.05, 1.075, 1.1. Black line connects points with maximum density for different temperatures. (b) Pressure as a function of density for different temperatures.

**Figure 5.** (a) The pseudo diffusion coefficient as a function of the temperature for several isochores and (b) the density for several isotherms. Black lines connects points with maximum and minimum of the pseudo diffusion coefficient.

**Figure 6.** Ratio of differently bonded water molecules for different isochores for (a) at temperature  $T^* = 0.16$ , (b) at  $T^* = 0.20$ .

**Figure 7.** (a) The translational order parameter as a function of the temperature for several isochores and (b) the density for several isotherms. Black lines connects points with maximum and minimum of the translational order parameter.

**Figure 8.** The distribution of the different order parameters for different isochores for (a) three fold parameter at temperature  $T^* = 0.15$ , (b) at  $T^* = 0.20$  and for (c) six fold parameter at temperature  $T^* = 0.15$ , (d) at  $T^* = 0.20$ .

**Figure 9.** (a) The orientational order parameter with three fold symmetry and (b) the orientational order parameter with six fold symmetry against density for several isotherms.

**Figure 10.** (a) The  $t - q_3$  order map and (b) the  $t - q_6$  plane.

**Figure 11.** (a) The pair entropy as a function of the temperature for several isochores and (b) the density for several isotherms. Black lines connects points with maximum and minimum of the pair entropy.

**Figure 12.** The pair correlation functions for different isochores for (a) at temperature  $T^* = 0.15$ , (b) at  $T^* = 0.20$ .

**Figure 12.** (a) The temperature-density plane containing all the anomalies found for

the 2D MB model of water. Colors of lines are explained by legend. (b) Same as in (a) but for pressure temperature plane.

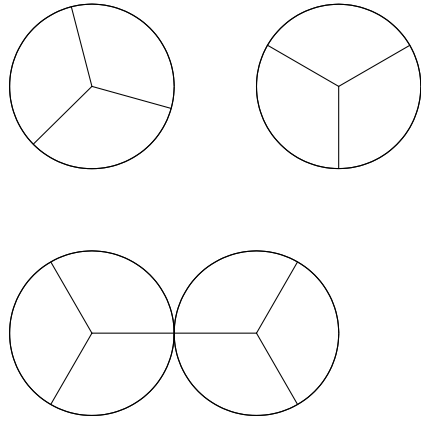
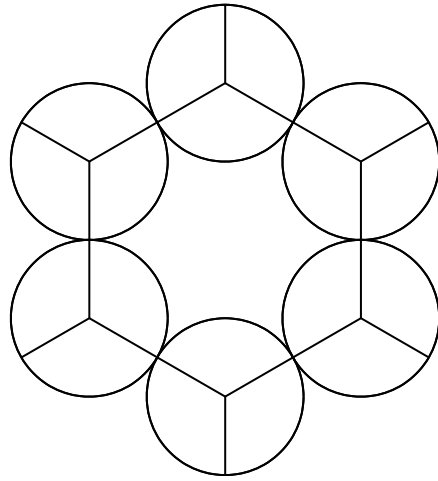
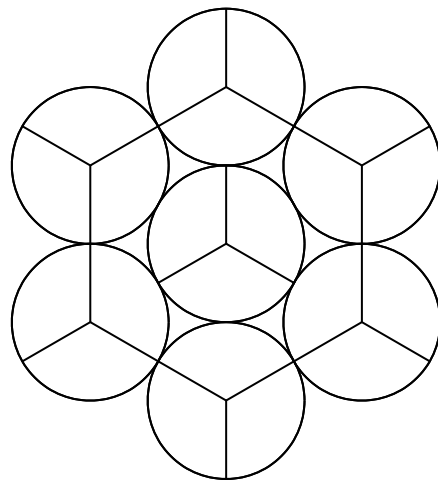


Figure 1 (Urbic et al.)



(a)



(b)

Figure 2 (Urbic et al.)

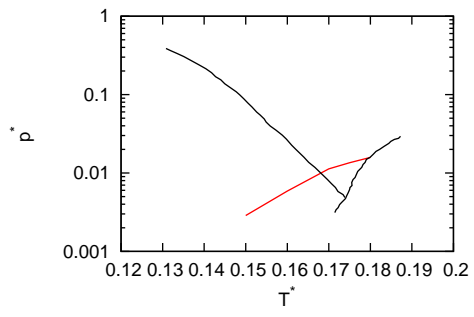


Figure 3 (Urbic et al.)

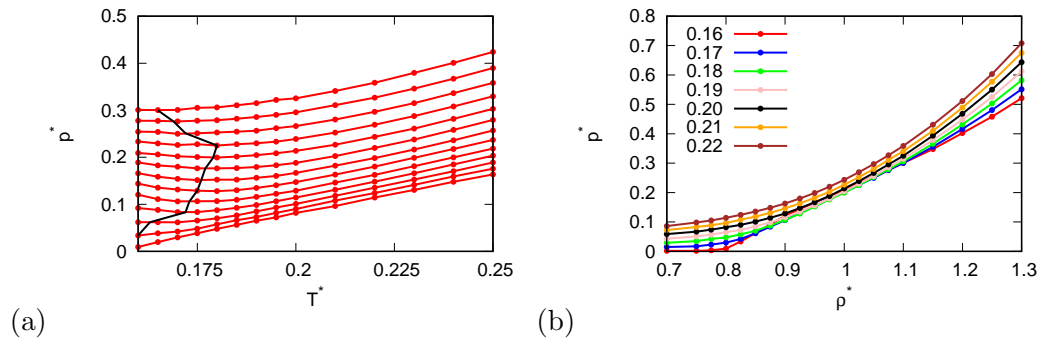


Figure 4 (Urbic et al.)

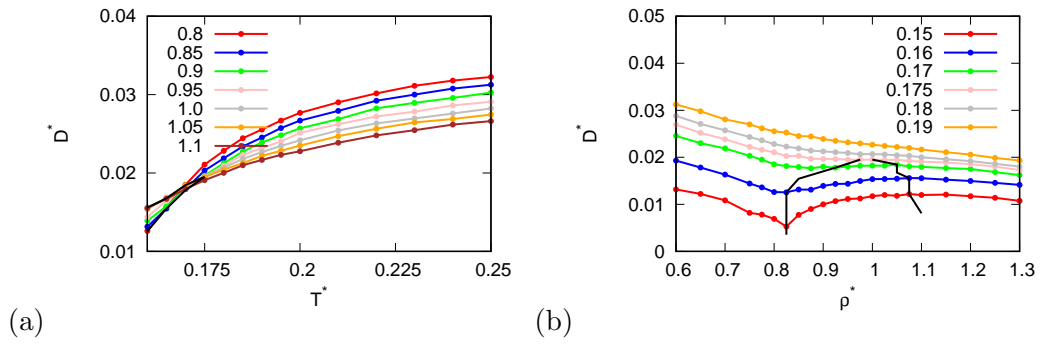


Figure 5 (Urbic et al.)

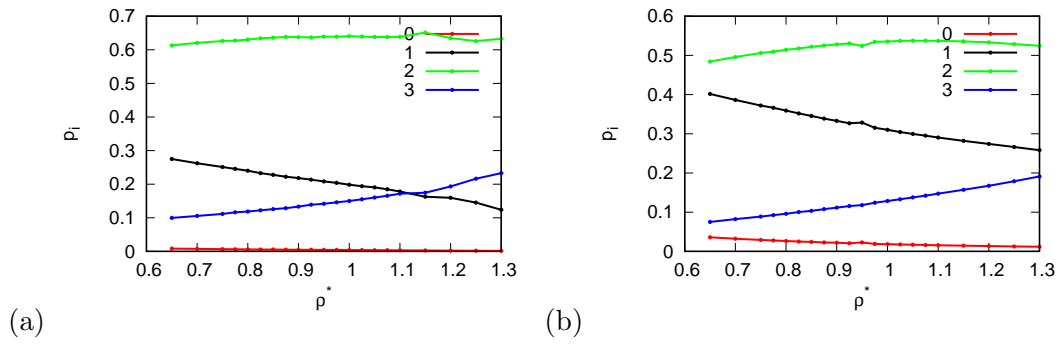


Figure 6 (Urbic et al.)

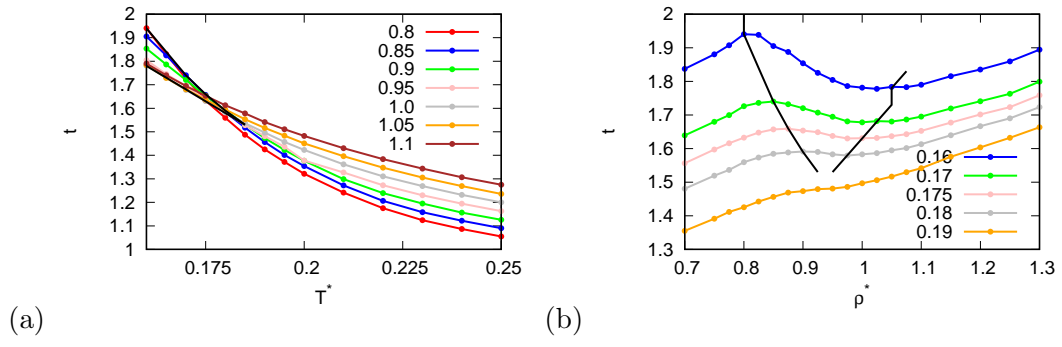


Figure 7 (Urbic et al.)

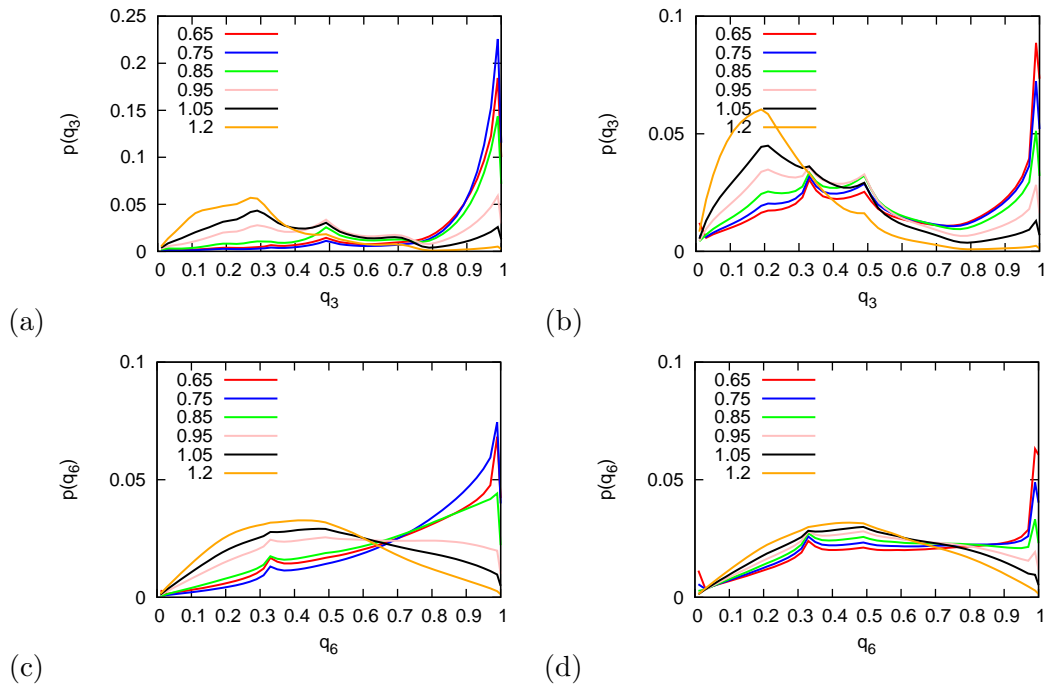


Figure 8 (Urbic et al.)

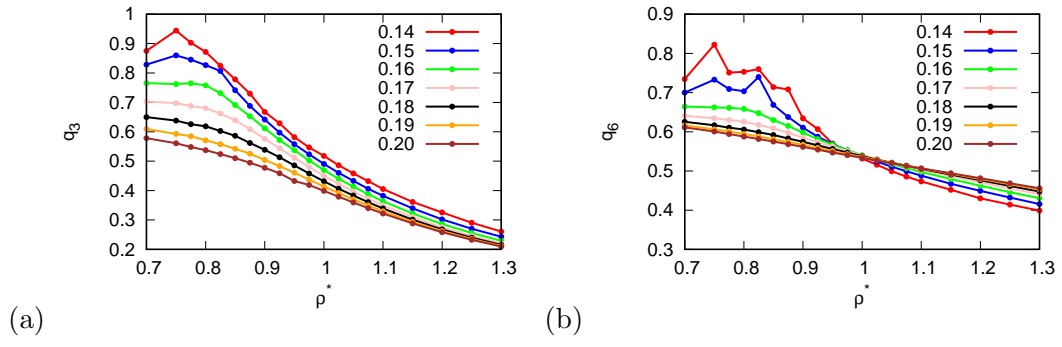


Figure 9 (Urbic et al.)

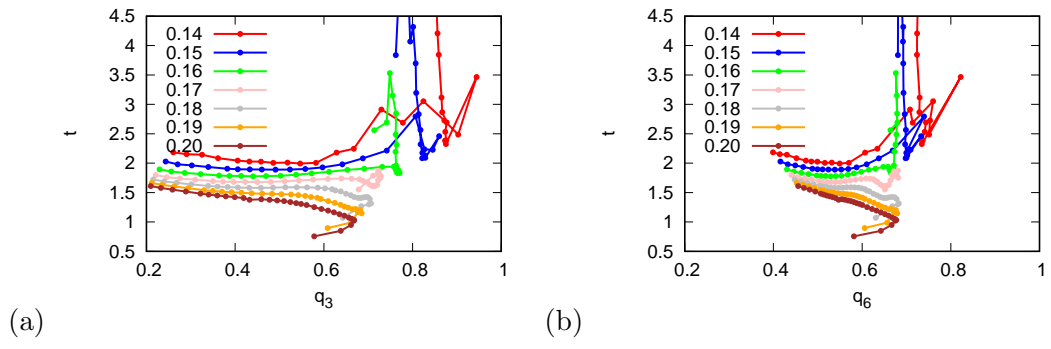


Figure 10 (Urbic et al.)

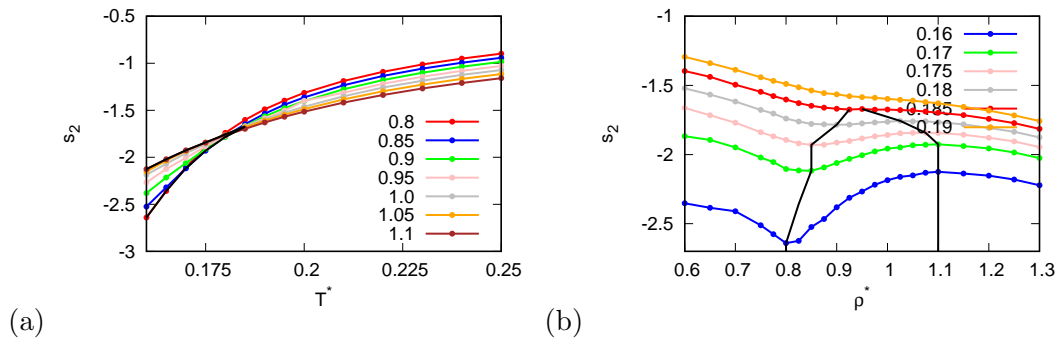


Figure 11 (Urbic et al.)

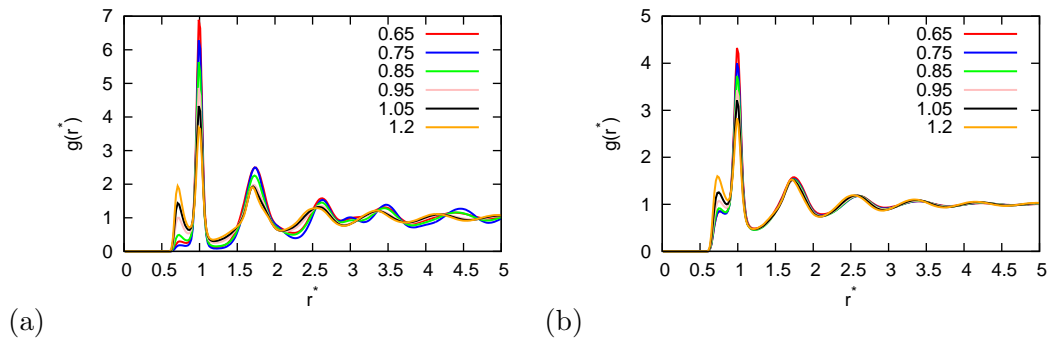


Figure 12 (Urbic et al.)

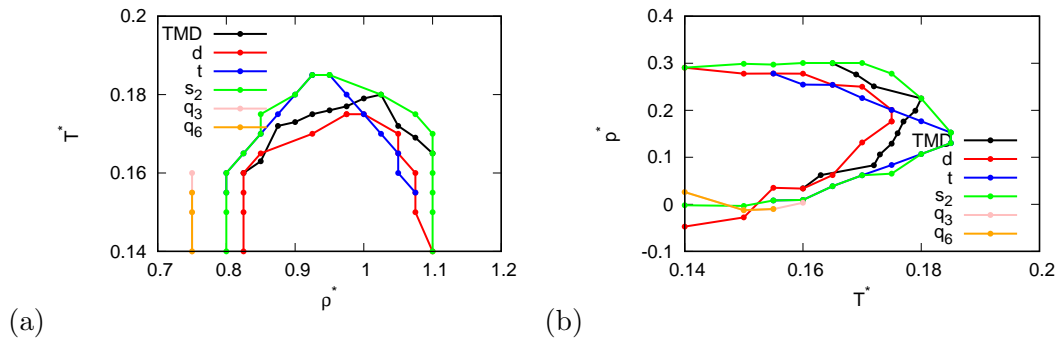


Figure 13 (Urbic et al.)